25th ABCM International Congress of Mechanical Engineering
October 20-25, 2019, Uberlândia, MG, Brazi

ENCIT 2019-1365
EXPERIMENTAL ANALYSIS OF THE RESTART FLOW OF A THIXOTROPIC FLUID IN PIPELINE

Roque Martins Duarte Junior[1]
Esther Maria Ihlenfeldt Rodrigues Santos[2]
Tainan Gabardo Miranda dos Santos[3]
Lucas Garcia Pereira[4]
Eduardo Matos Germer[5]
Cezar Otaviano Ribeiro Negrão[6]
Research Center for Rheology and Non-Newtonian Fluids (CERNN)
Postgraduate Program in Mechanical and Materials Engineering (PPGEM)
Federal Technological University of Paraná (UTFPR)
Deputado Heitor Alencar Furtado St., n. 5000, CEP: 81280-340 Curitiba-PR-Brazil.
roquemdjunior@gmail.com[1], esther@alunos.utfpr.edu.br[2], tainansantos@utfpr.edu.br[3], lucper.2016@alunos.utfpr.edu.br[4], eduardomg@utfpr.edu.br[5], negrao@utfpr.edu.br[6].

Abstract. *Oil exploration in ultra-deep waters has increased recently due to recent discoveries of new basins in offshore fields. The rise in offshore production led to an increase in paraffinic oil extraction. During oil transportation from the reservoirs to the seashore, the oil losses heat to the ocean floor. The temperature difference induces the cooling of the oil causing increase of the solubility and precipitation of paraffin crystals, which may lead to oil gelation on the production line during shutdowns. This gelled material exhibits several non-Newtonian fluid characteristics, such as viscoplasticity, elasticity, time dependence, thermal and shear dependence. To restart the flow under these conditions, it is necessary to impose pressures higher than the usual ones. If not controlled, pressure too high may damage the pipeline and cause environmental and financial problems. Therefore, the objective of this paper is to investigate how the time dependence affects the restart pressures. To do so, the flow curve, flow start-up tests with different resting times and start-up visualization were performed. The fluid used will be an aqueous solution of Laponite (2% wt.), which was studied on a laboratory-scale flow loop (long helical pipe) with thermal control. The results of the flow curve showed that the fluid had a shear-thinning behavior. The visualization experiment indicated a higher yield shear stress to start-up the flow. Finally, it was highlighted that the resting time has a considerable influence over the overshoot pressures during the flow start-up.*

Keywords: *flow loop, flow start-up, Laponite, non-Newtonian fluid.*

1. INTRODUCTION

The search for new oil reservoirs has led offshore exploration to reach ultra-deep regions. According to ANP (2019), the offshore oil production accounted for 93.9% of the Brazilian production in December of 2018 following the trend of the previous months. There is a tendency for deep water and ultra-deep-water production to meet most of the energy demand in the coming years, due to the recent oil discoveries in offshore fields that correspond to 150 million barrels of oil, while onshore reserves correspond to only 25 million barrels (Chala et al., 2018).

Exploitation in ultra-deep waters has increased oil production tremendously and, consequently, increased the production of paraffinic oil (Li et al., 2015). These crude oils have high molecular weight paraffins, i.e., n-paraffin of straight chain and iso-paraffin of branched-chain, which are one of the main flow assurance problems encountered during production and transportation (de Souza Mendes and Thompson, 2012). Due to the high content of paraffin in its composition, the transport of waxy crude oil through the seabed is a challenging and costly task.

A common problem encountered during transportation is the precipitation and deposition of paraffin crystals in the pipeline, which occurs when the oil temperature reaches its crystallization temperature (Kané et al., 2003; Venkatesan et al., 2005). The precipitation leads to the accumulation of paraffin crystals on the internal surface of the pipelines, and it may cause an increase in the pressure loss and decrease of the flow rate. Moreover, a continuous deposition of paraffin may result in pipeline blockage (Chala el al., 2018).

The buildup of the gelled structure occurs in eventual shutdowns of production and transportation of the waxy crude oil. It is emphasized that for the gel to be formed only 0.5% of precipitated paraffin is necessary (Yao et al., 2016). When the oil is gelled in the pipeline, high pressures are required to break the gel and to start-up the flow (Magda et al.,

2013). Therefore, accurate prediction of pressures required to start the flow is important, since overestimating the pressure requires the use of more robust pipes, which will make the project unfeasible (Fossen et al., 2013). In addition, if the minimum restart pressures are not reached (underestimating the pressure), the flow will not restart and it will lead to large financial losses.

Waxy crude oils exhibit several non-Newtonian characteristics, such as: viscoplasticity, elasticity, time dependence and dependence of thermal and shear histories (Tarcha et al., 2015). These characteristics added to the composition present in the gelled structure influence the complexity of the behavior of the material during the flow restart.

In order to isolate a single characteristic of the overall behavior of waxy crude oil, some authors investigated the start-up phenomena with yield-stress materials (Pereira, 2018; Abedi et al., 2019). Others investigations using a thixotropic yield stress material (Laponite RD) were carried out by Escudier et al. (1995), Escudier and Presti (1996), Corvisier et al. (2001), Taghipour et al. (2012), Balvedi (2017), Pereira (2018) and Abedi et al. (2019) to evaluate the reversible temporal dependence behavior of the fluid. Most of these studies were performed through rheometry, and there are still few studies reported in the literature using experimental apparatus. Thus, it is important to evaluate the rheology of this material by an experimental apparatus since it has more similar conditions to the real ones.

Therefore, this paper discusses the influence of the thixotropic behavior over the fluid start-up by evaluating different resting times. In order to achieve the objective, a laboratory-scale flow loop was used to conduct te following testes: flow curve, flow restart with different resting times and start-up visualization experiments.

2. MATERIALS AND METHODS

The tests were performed with an aqueous solution of Laponite RD. The formulated fluid was tested in a laboratory-scale flow loop that is compound of two syringe pumps, a long helical pipe, a fluid reservoir, four pneumatic valves and four pressure transducers. All the components are placed inside a temperature-controlled chamber.

2.1 Working fluid

Laponite RD is a synthetic clay mineral, which has a nanometric shape with non-uniform electric charge distribution (Jatav and Joshi, 2014). When dispersed in water, this material exhibits shear-thinning, slightly viscoelastic and thixotropic behavior (Escudier and Presti, 1996). Tanaka et al. (2014) and Abedi et al. (2019) reported that the addition of 10^{-3} M of salt (NaCl) in the Laponite suspension (with pH = 10) enhance the ionic strength and the yield stress of the material. Therefore, the aqueous suspension of Laponite of this study was prepared with 2% weight concentration and 10^{-3} M of salt (NaCl). The pH sample was at 10, so no additional adjustment was necessary.

2.2 Experimental Setup

The main components of the flow loop were the reservoir and the two syringe pumps that were connected to a long helical pipeline and a small one, namely bypass. Figure 1 shows a schematic diagram of the experimental apparatus, where can also be seen the four pressure transducers (P1 to P4) and ten uniformly distributed thermocouples (T) were placed along the pipeline. All the equipment was placed inside a thermally insulated chamber to control the temperature during the tests.

The flow loop (Fig. 1) was operated with two syringe pumps that could provide constant flow rate by working simultaneously or individually. For the tests, the normal condition was to use it in the individual mode, i.e., while one of the pumps was being filled with fluid, the other one was pumping. After the pump, two possible paths (helical pipeline or bypass) were available depending on the test performed. Then, the fluid returned to the reservoir. The flow direction along the circuit is represented by the arrows in Fig. 1.

Both syringe pumps (model 500D) were manufactured by Teledyne ISCO™. The set of pumps works with a flow rate ranging from 0.001 to 204 ml/min, and accuracy of ± 0.5%. The desired flow rate is set up by the user in an external controller which allows pneumatic actuation of the ball valves V1, V2, V3 and V4 to fill or empty the pumps.

The helical pipe has a length of 50.53 meters and an inner diameter of 10 mm, while the bypass line has a capillary tube (CT) with a length of 1.2 meters and inner diameter of 2.03 mm. It should be highlighted that the bypass allows the control and imposition of higher pressures along the pipeline.

The absolute pressure transducers (P1 to P4) were manufactured by HBM™, P3 Industrial Class model with a maximum pressure of 20 bar and an accuracy of 0.03 bar. These transducers have an internal resistance thermometer (RTD), which was used as a reference to the fluid temperature control. The distance between P1 and P2, P3 and P4 were 11.03, 22.06 and 33.16 m, respectively. P4 was 8.63 meters from the pipeline outlet.

The LabVIEW 2016™ software was used for data acquisition. Furthermore, the software utilized a PID controller to achieve and maintain the desired average temperature for the experiments, by using a set of electrical resistances and a refrigeration unit. The average temperature was calculated by the average temperatures measured with ten thermocouples (T) displaced along the pipe surface and the RTD (PT100) which was assembled inside the reservoir.

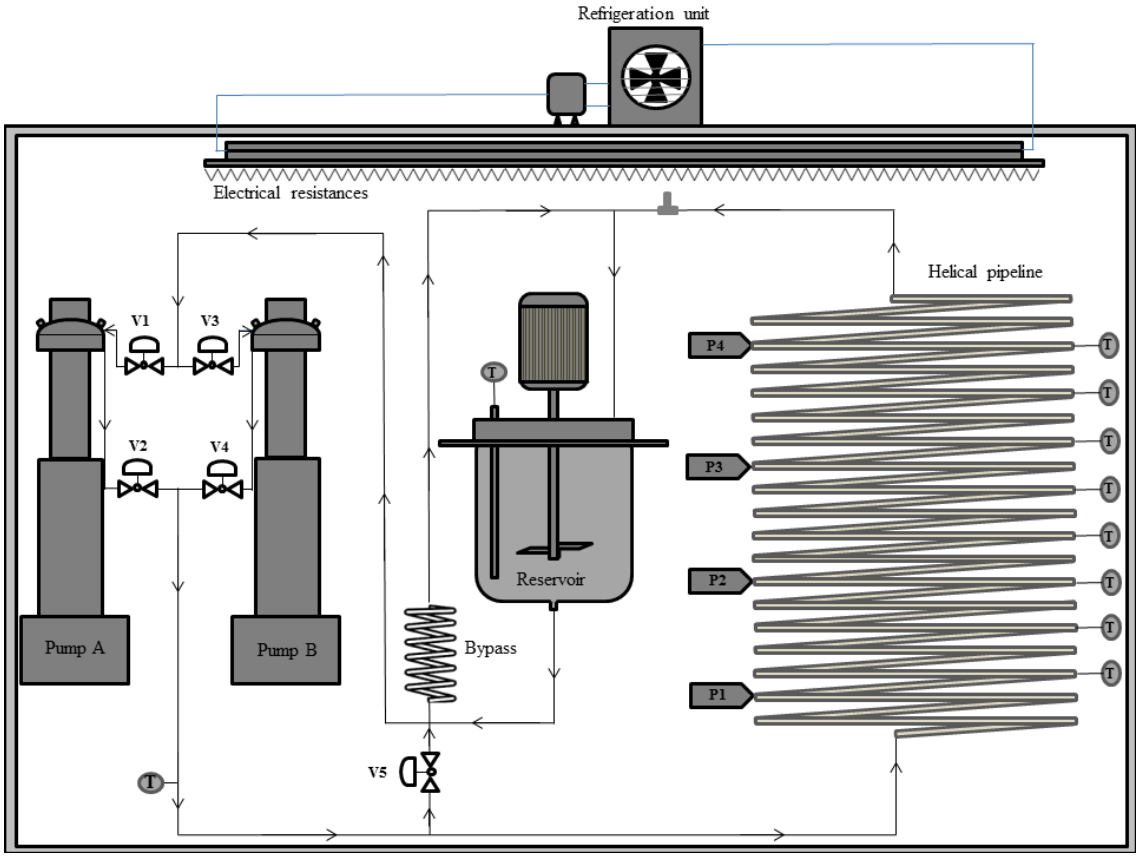

Figure 1 - Schematic diagram of the laboratory-scale flow loop.

2.3 Experimental procedures

Before any experiment, a pre-test was conducted: (a) the fluid was pumped at constant flow rate for 90 minutes until it reached the initial standard test pressure condition as the test temperature was set and maintained uniform throughout the flow loop; (b) all the valves (V1 to V4) were opened, so the pipeline achieved an initial non-zero pressure distribution due to the residual stress of the material; (c) and then the test starts to be recorded. Both steps (b) and (c) last 30 s before every test.

The following tests were accomplished in controlled temperature of 25 ºC and all the experiments were performed in triplicate to assure repeatability.

2.3.1) Flow curve

The flow curves were performed in the rheometer and in the flow loop for comparison purposes.

a) Rheometer

The rheometer used was a HAAKE (model MARS III) with concentric cylinder geometry and gap of 1 mm. The procedure used was the imposition of decreasing steps of shear rates with minimum duration of 1500 s each one. The shear rates were imposed in the following sequence: 100, 50, 25, 5, 1 and 0.1 s^{-1}.

The tests were performed using a Laponite sample taken from the flow loop on the same day the tests were performed, in order to evaluate the sample with the same degree of structuration. Besides that, to avoid evaporation of the sample during the test, a thin layer of lubricant oil was put over the sample.

b) Laboratory-scale flow loop

The procedure was to set up the flow rate in the pumps controller, after the pre-test. Then, the pressure evolution profile was recorded until it reached the equilibrium pressures. The selected flow rates were 0.644 6.44, 32.2, 64.4, 128.8 and 193.2 ml/min. It is highlighted that for a Newtonian fluid, these flow rates values correspond to shear rates of 0.1, 1, 5, 10, 20 and 30 s^{-1}, respectively.

From the equilibrium pressures, the flow curve can be obtained by the relation of wall shear stress (τ_w) and the Weisserberg-Rabinowitsch wall shear rate ($\dot{\gamma}_{wr}$). These parameters were calculated by applying the following equations:

$$\tau_w = \frac{D\Delta P_{1-4}}{4L_{1-4}} \tag{1}$$

where D is the inner diameter, ΔP_{1-4} is the pressure difference between the pressure transducer 1 (P1) and 4 (P4), L_{1-4} is the distance between P1 and P4, and,

$$\dot{\gamma}_w = \frac{32Q}{\pi D^3} \tag{2}$$

where $\dot{\gamma}_w$ is the wall shear rate for Newtonian fluids and Q is the volumetric flow rate. Eq. 3 is known as Weissenberg-Rabinowitsch equation, and it is used to correct the wall shear rate ($\dot{\gamma}_{wr}$) considering the flow effects of non-Newtonian fluids (Macosko, 1994), such the fluid used in this study.

$$\dot{\gamma}_{wr} = \frac{\dot{\gamma}_w}{4}\left(3 + \frac{d\ln Q}{d\ln \tau_w}\right) \tag{3}$$

2.3.2. Flow start-up with inlet constant flow rate

The objective of this test was to assess the influence of the resting time over the material overshoot pressure. So, the main focus of this experiment was on the transient region of pressure evolution.

To perform this experiment, valve V5 from the bypass line remained closed, so the fluid flowed only through the helical pipe. After the pre-test, the selected resting time was awaited, and then the start-up was initiated while the pressure profiles were recorded. The resting times of 0.5, 1, 10 and 30 min were evaluated for the following flow rates of 0.644, 6.44 and 64.4 ml/min.

2.3.3. Visualization of the start-up flow

This test was performed to verify if the pressure difference calculated by the yield stress (Eq. 1) is in fact the minimum pressure required to flow the material. The material yield stress was obtained by the HB fit equation of the flow curve.

In this case, valve V5 remains open allowing the fluid to flow through both the bypass and the helical pipeline. The bypass was designed to have a lower head loss than helical pipeline, so that fluid would flow preferentially through it. However, when a flow equivalent to the yield stress is imposed, the fluid is also expected to flow through the serpentine. Thus, the pressure imposed at the helical pipeline inlet is controlled indirectly, as the fluid flows through the bypass pipe. The flow visualization is achieved through a webcam installed between the end of the serpentine and the "T" connection, where the evolution of the fluid displacement was observed by means of a transparent hose attached to connection T. The hose is marked with lines every 2 mm to estimate how much the fluid displaces itself.

In this test flow rates between 9.33 to 35.42 ml/min were applied, in order to determine the shear stress that start-up the flow and, then it was observed if the fluid would flow. The resting time for these tests was 1 min.

3. RESULTS AND DISCUSSION

This section presents the results of the flow curve, the flow start-up with constant flow rate and the restart visualization obtained using the procedures described above.

3.1. Flow curve

For the following results, the Herschel-Bulkley (HB) equation (Eq. 4) was used to fit the experimental data by the least square method as

$$\tau = \tau_0 + k\gamma^n \tag{4}$$

where τ_0 is the yield stress, k is the consistency index and n is the flow index.

The flow curve shown in Fig. 2 shows the shear stress results obtained with the flow loop (red) and the rheometer (black). The symbols represent the experimental results and the bars the standard deviation of the triplicate. The lines represent the Herschel-Bulkley fit.5

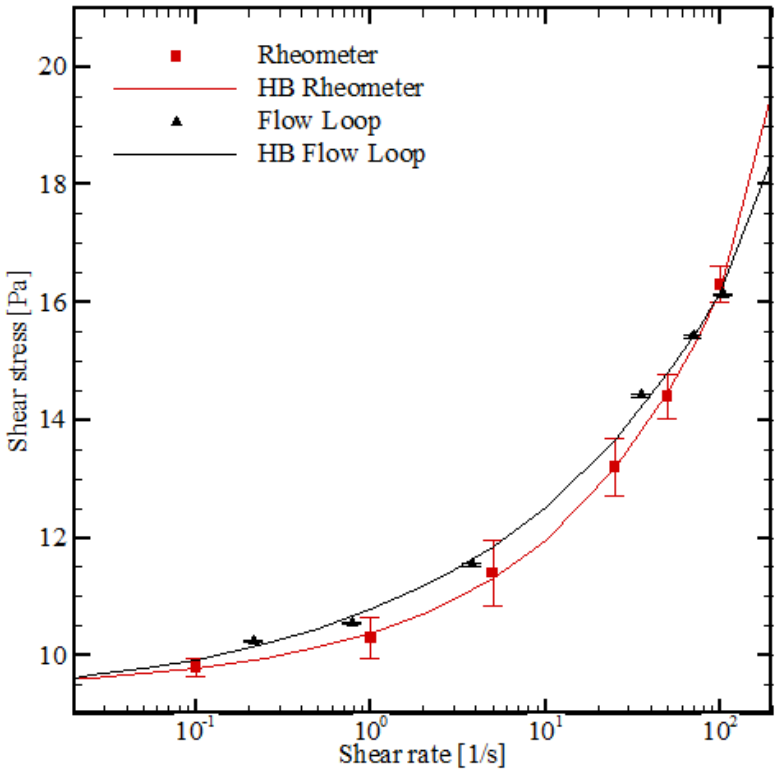

Figure 2. Comparison of Laponite (2%) flow curves obtained with the flow loop and the rheometer.

As it can be seen in Fig. 2, the material in the steady-state has a shear thinning behavior and tends to a yield stress for both cases. Besides that, there is a good agreement between the flow loop and rheometric results. Nevertheless, the standard deviation of the rheometer was higher, indicating that the flow loop had a better repeatability.

The HB equation for the experimental flow loop was $9.16+1.61\dot{\gamma}^{0.32}$ with a maximum standard deviation of 0.02 Pa for 35.5 s^{-1}. For the rheometer, the HB equation was $9.4+1.01\dot{\gamma}^{0.4}$ and it had a maximum standard deviation of 0.55 Pa for 5 s^{-1}. The coefficient of determination (R^2) for both HB equations was 0.99 and the maximum percentage difference between these fit equations was 4.82% for 5 s^{-1}.

3.2. Visualization of the start-up flow

Initially, in order to determine the flow rate necessary to promote a shear stress equivalent to the yield stress, tests with increasing flow rates of 3.22 ml/min were performed for 20 min for each flow rate, starting with 9.66 up to 35.42 ml/min. In these tests, the measured pressures were indirectly controlled by the imposed flow rate, as the fluid flowed only through the bypass until the shear stress along the pipeline reached the yield stress, promoting flow also through the helical pipeline. The tests were performed with the "T" connection open, so that the flow start-up could be visually confirmed.

For the flow rates below 32.2 ml/min, it was observed that the fluid displaced a few millimeters in the hose as soon as the overshoot were observed, but then stopped, i.e., besides the initial flow start-up, the steady-state shear stress in the material structure did not reach the minimum value to promote a continuous flow.

Fig. 3 shows the shear stress between P1 and connection T for the flow rates of 32.2 and 35.42 ml/min. For 32. 2 ml/min, the overshoot has reached 8.2 Pa, which is 10% lower than the yield stress obtained with the HB fit (9.16 Pa). After that, the shear stress falls to 7.8 Pa and it starts to rise towards to 9.7 Pa, where the shear stress value seems to reach an equilibrium state until the end of the test.

For flow rate of 35.42 ml/min the start-up has occurred. As shown in Fig. 3, the shear stress has reached 9.0 Pa in the overshoot, which is 2% lower than the yield stress of the HB fit. After the overshoot, the yield stress falls to 8.2 Pa and it starts to rise towards 10.2 Pa. Starting-up the flow with low and similar shear stress when compared to the yield

stress obtained through Eq. 1 was already expected since this equation considers the flow as viscous, incompressible and one phase only (Chala et al., 2018).

It is interesting to note that both shear stress curves have a similar behavior, and nevertheless, flow was observed only for one case. First, the material structure breaks in the overshoot, causing the shear stress to reduce. Then, the shear stress increased as the fluid started to restructure until it reached the steady state. For both shear stress curves, besides the low overshoot value when compared to the HB fit, the start-up initiated. However, only the flow rate of 35.42 ml/min had a continuous flow, which indicates that the steady-state shear stress value is determinant to maintain a continuous flow in the start-up, which in this case was around 10.2 Pa. Therefore, the required shear stress to start-up the flow for this test is considered to be between 9.7 and 10.2 Pa.

The shear stress that started the flow for the visualization test is bit larger than the estimated through the flow curve. A reasonable explanation is that the minimum strain rate used in the flow curve was not low enough, which would probably lead to a larger yield shear stress value, and consequently it would probably be close to the one from this test. The flow curve did not performed tests with lower strain rates due to the time required to reach steady-state.

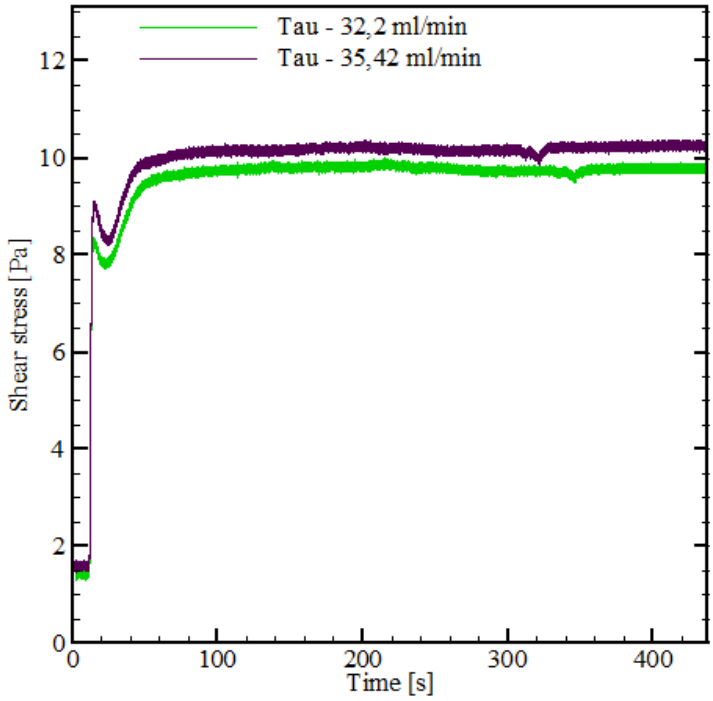

Figure 3. Shear stress evolution between P1 and connection T for flow rate of 32.2 and 35.42 ml/min.

Fig. 4 presents pictures regarding different times of the start-up flow for the flow rate of 35.42 ml/min, where can be noted that the fluid displaced itself through the hose attached to connection "T" (Fig. 4a to 4e). The start-up flow initiated in the overshoot around 15 s, however it is when the shear stress reaches the steady-state around 40 s that the fluid starts to displace itself at higher flow rates, indicated by Fig. 4b to 4f. As seen in Fig. 4, the fluid moved along the hose which indicated in fact that the start-up flow occurred. The fluid displaced itself more than 28 mm during 300 s of the test and then fluid level reached the hose outlet, as seen in Fig. 4e.

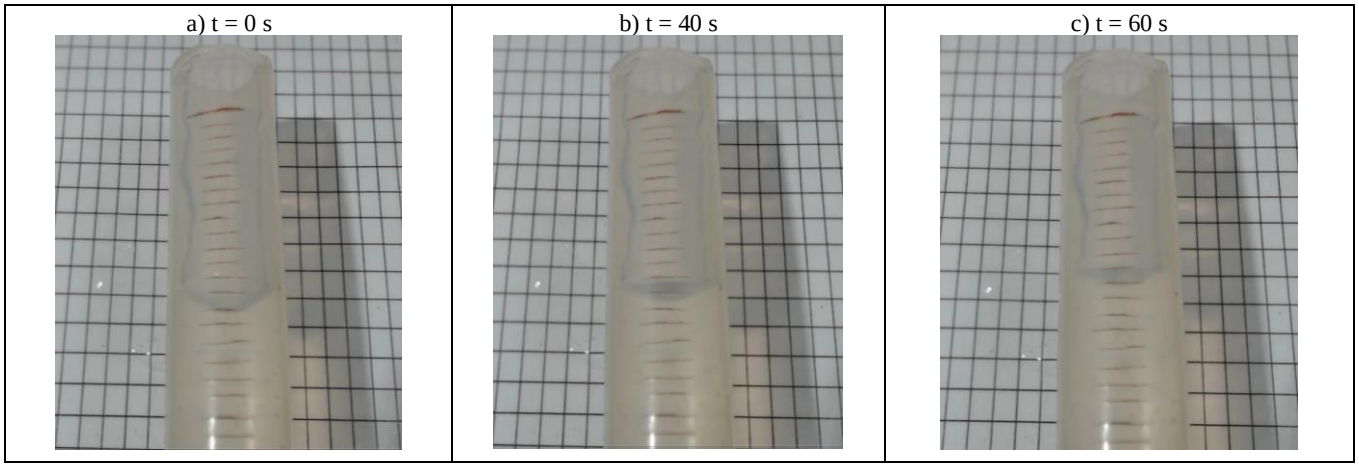

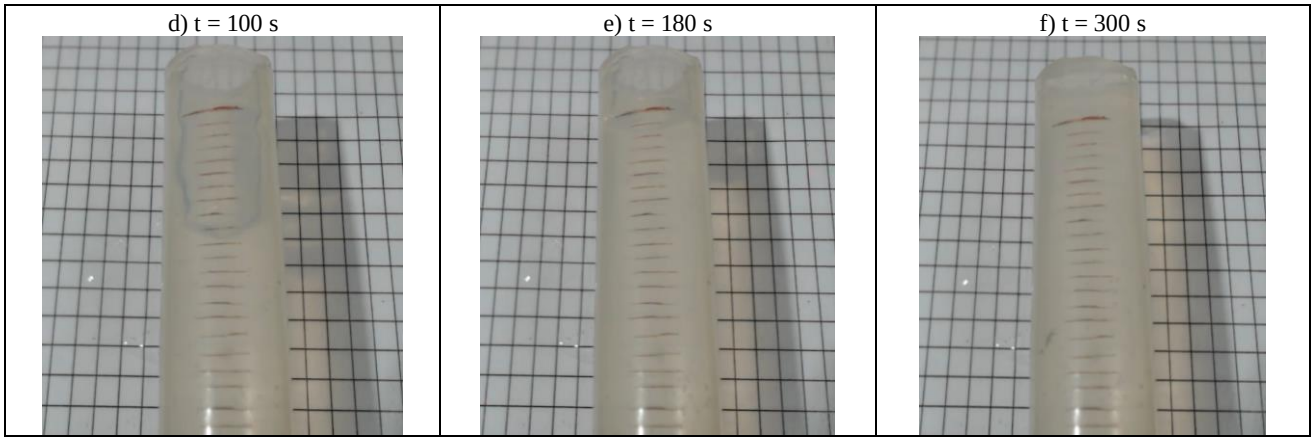

Figure 4. Images of the start-up flow for flow rate of 35.42 ml/min. a) Fluid in the initial position; b) Fluid started to displace itself a soon as the overshoot occurred; c) Fluid after displacement of 4 mm; d) Fluid after displacement of 8 mm; e) Fluid after displacement of 25 mm; f) Fluid overflow outside the hose;

3.3 Flow start-up with inlet constant flow rate

In this subsection, first the results for different flow rates regarding a resting time of 30 s are presented, and then the influence of the resting time over the pressure evolution is analyzed.

Fig. 5 shows the pressure evolution of transducer P1 for different flow rates. It can be seen that for a thixotropic material, an increase in the imposed flow rate has led to an increase in the overshoot pressures, and also in the steady-state pressure level. These overshoots are not linearly proportional to the flow rate increase, as exhibited in the measured pressure at P1.

As observed in Fig. 5, the overshoot time depends on the flow rate. The higher the flow rate, faster the overshoot, consequently, more quickly the material flows. It seems that for a determined range of high flow rate ($\geq$ 64.4 ml/min) the start-up tends to occur in less than 0.5 s, however for lower flow rates it takes more than 7 s.

The time difference between flow rates is due to the inertia and the viscous dissipation of the material. As the flow rate gets lower, lower the ratio between inertia and viscous dissipation, which results in a delayed flow start-up. For higher flow rates, the opposite is observed.

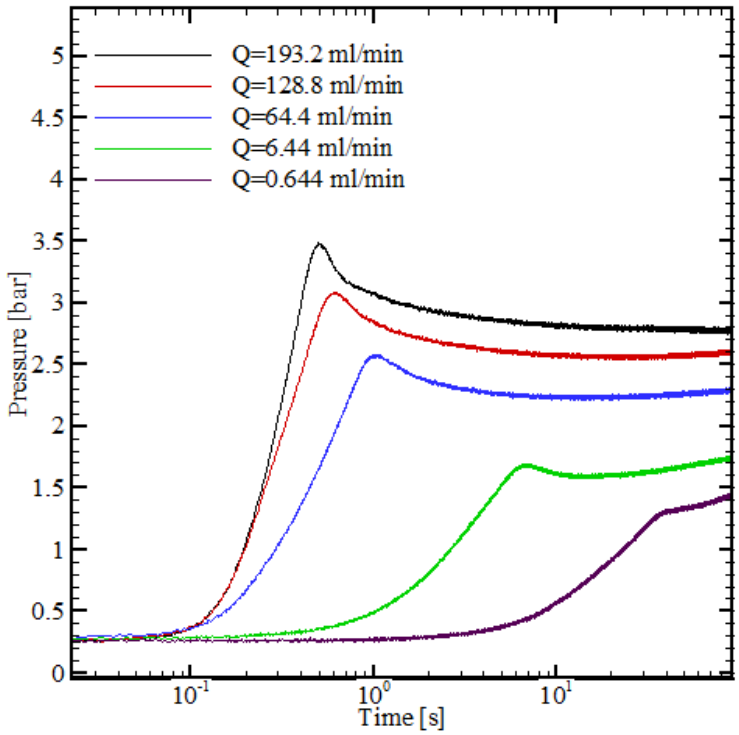

Figure 5. Overshoot pressure of P1 for different imposed flow rates with resting time of 30 s.

The influence of the resting time over the restart pressure is presented in Fig. 6 and Table 1. Fig 6 presents the pressure evolution measured in P1 for the flow rate of 6.44 ml/min with the resting times of 0.5, 1, 10 and 30 min. Note that as the resting time increases, the time to occur the overshoot and its value also increases.

The increase in the resting time allows the material to strengthen its structure and delay the restart flow. When comparing the lower resting times (0.5 and 1 min) it is observed that there is already a difference in the transient part in the pressure evolution, which may indicate that the changes in the material structure happens very quick. The test with 1 min of resting time had an overshoot 18% higher when compared to resting time of 0.5 min.

Note that tests with longer resting times (10 and 30 min) have a steeper slope at the beginning of the transient regime (2 – 6 s), which suggests that the increase in the resting time may induce the appearance of a higher elasticity, as a consequence of the greater restructuring of the material.

For the resting time of 30 min, the pressure curve presented oscillations during the rise to the overshoot (Fig. 6), which is believed to be due to the bubbles that are present in the fluid. By observing the samples taken from the apparatus, it was noticed that when the material stayed at rest, the smaller bubbles assembled into larger bubbles. It is pointed out that these bubbles may change the material's compressibility and the pressure evolution in the transient regime, as observed in the last seconds of the transient regime (6 – 15 s).

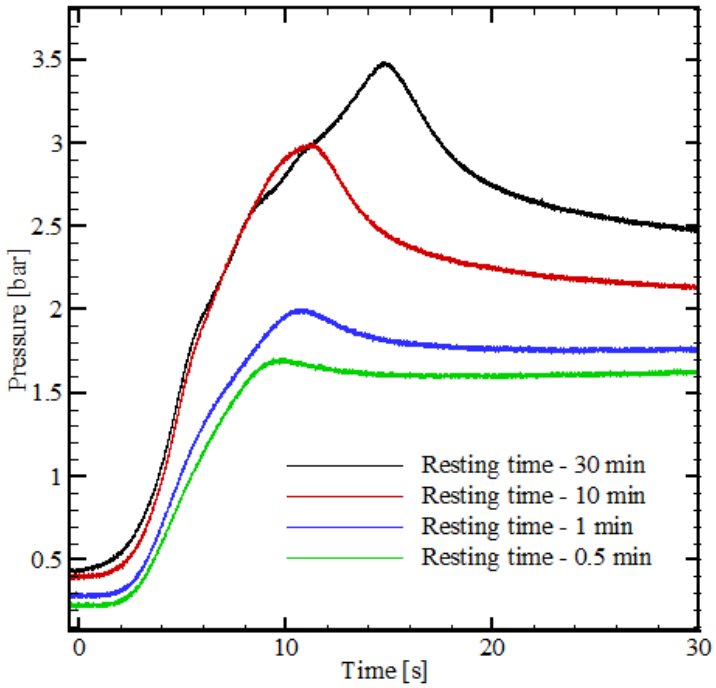

Figure 6. Influence of resting time on overshoot pressure of P1 for flow rate of 6.44 ml/min.

Table 1 compares the overshoot time and the overshoot and steady-state pressures for the flow rates of 0.644, 6.44 and 64.4 ml/min regarding the resting times of 0.5, 1 and 10 min.

In general, for each flow rate tested, it is seen that as the resting time is incremented the time required to the overshoot occur and the overshoot pressure also increase. However, the steady-state pressure value is independent of the resting time. The differences in obtained results for the steady-state pressure are within the experimental flow loop uncertainties.

Note that for the flow rate of 6.44 ml/min with the resting time of 10 min, the time to the overshoot occur is slightly lower than for 1 min. This is probably due to the influence of the bubbles that changes the compressibility of the material in the transient regime, as shown in Fig 6.

The tests performed here showed that the longest the resting time, the higher the pressure required to break up the material structure. Therefore, it indicates that the resting time of a thixotropic material has direct influence on the time and overshoots pressures during the restart flow.

Table 1. Influence of resting time on the overshoot time, overshoot pressure and steady-state of the transducer

Flow rates	Resting time of 0.5 min		
	Overshoot time	Overshoot	Steady-state
64.4 ml/min	10.3 s	2.57 Pa	2.41 Pa
6.44 ml/min	17.5s	1.68 Pa	1.92 Pa
0.64 ml/min	76.6 s	1.46 Pa	1.76 Pa

	Resting time of 1 min		
	Overshoot time	Overshoot	Steady-state
64.4 ml/min	11.8 s	2.79 Pa	2.41 Pa
6.44 ml/min	24.3 s	1.98 Pa	1.93 Pa
0.64 ml/min	209 s	1.86 Pa	1.81 Pa
	Resting time of 10 min		
	Overshoot time	Overshoot	Steady-state
64.4 ml/min	14.2 s	3.95 Pa	2.43 Pa
6.44 ml/min	23,6 s	3.02 Pa	1.99 Pa
0.64 ml/min	227,4 s	2.13 Pa	1.83 Pa

In general, for each flow rate tested, it is seen that as the resting time is incremented the time required to the overshoot occur and the overshoot pressure also increase. However, the steady-state pressure value is independent of the resting time. The differences in obtained results for the steady-state pressure are within the flow loop uncertainties.

Note that for the flow rate of 6.44 ml/min with the resting time of 10 min the time to the overshoot occur is slightly lower than for 1 min. This is probably due to the influence of the bubbles that changes the compressibility of the material in the transient regime, as shown in Fig 6.

The tests performed here showed that the longest the resting time, the higher the pressure required to break up the material structure. Therefore, it indicates that the resting time of a thixotropic material has direct influence on the time and overshoots pressures during the restart flow.

4. CONCLUSION

The complexity of the rheological behavior of crude oils allows these fluids to have a variety of uncommon characteristics. During the flow restart process, the characterization of these properties is even more problematic due to the coexistence of such characteristics with different operational conditions. To better understand the thixotropic influence in the waxy oils behavior, this paper used an experimental apparatus to study the start-up flow of Laponite RD (2% wt.), in order to isolate the thixotropic effect.

The results of both flow curve (rheometer and flow loop) indicated a shear thinning behavior in the steady-state regime. The Hershel-Bulkley fit and the comparison between the flow loop and rheometer results showed a good agreement.

The visualization test showed that the minimum shear stress to promote the flow start-up is lower than the obtained through the Hershel-Bulkley fit. Besides that, it was highlighted that not only the overshoot but also the steady-state shear rate is important to promote a continuous flow. This test was preliminary and further work will be performed with longer waiting times.

The evaluation of the resting time over the overshoot pressure and the time that it occurred showed clearly the influence of this parameter in a thixotropic material during the restart flow.

5. ACKNOWLEDGEMENTS

The authors acknowledge the financial support of PETROBRAS S/A and ANP (Brazilian National Oil Agency).

6. REFERENCES

Abedi, B., Mendes, R., de Souza Mendes, P.R., 2019. “Startup flow of yield-stress non-thixotropic and thixotropic materials in a tube”. *J. Petrol. Sci. Eng.* 174:437–445.

ANP, 2019. Boletim da Produção de Petróleo e Gás Natural. 09 Feb. 2019 <http://www.anp.gov.br/images/publicacoes/boletins-anp/Boletim_MensalProducao_Petroleo_Gas_Natural/boletim-dezembro-2018.pdf>.

Balvedi, G.A.S., 2017. *Avaliação reológica experimental do comportamento tixotrópico de uma solução de Laponita-RD®*. Monography, Federal Technological University of Paraná, Curitiba-PR, Brazil.

Chala, G.T., Sulaiman, S.A. and Japper-Jaafar, A., 2018. “Flow start-up and transportation of waxy crude oil in pipelines-A review”. *Journal of Non-Newtonian Fluid Mechanics*, Elsevier, 251: 69–87.

Corvisier, P., Nouar, C., Devienne, R., Lebouché, M., 2001. “Development of a thixotropic fluid flow in a pipe”. *Exp. Fluids* 31:579–587.

de Souza Mendes, P.R., Thompson, R.L., 2012. “A critical overview of elasto-viscoplastic thixotropic modeling”. *J. Non Newtonian Fluid Mech.* 187–188: 8–15.

Escudier, M., Presti, F., 1996. “Pipe flow of a thixotropic liquid”. *J. Non Newtonian Fluid Mech.*, 62:291– 306.

Escudier, M.P., Gouldson, I.W., Jones, D.M., 1995. “Flow of shear-thinning fluids in a concentric annulus”. *Exp. Fluids* 18:225–238.

Fossen, M., Øyangen, T., Velle, O.J., 2013. "Effect of the Pipe Diameter on the Restart Pressure of a Gelled Waxy Crude Oil". *Energy & Fuels*, 27(7): 3685–3691.

Jatav, S., Joshi, Y.M., 2014. "Chemical stability of Laponite in aqueous media". *Appl. Clay Sci*. 97– 98:72–77.

Kané, M., Djabourov, M., Volle,J.-L., Lechaire, J.-L., Frebourg, G., 2003. "Morphology of paraffin crystals in waxy crude oils cooled at quiescent condition and under flow". *Fuel* 82:127-135.

Li H., Zhang J., Song C, Sun G., 2015. "The influence of the heating temperature on the yield stress and pour point of waxy crude oils". *J. Petrol. Sci. Eng.* 135:476–483.

Magda, J.J., Elmadhoun, A., Wall, P., Jemmett, M., Deo, M.D., Greenhill, K.L., Venkatesan, R., 2013. "Evolution of the Pressure Profile during the Gelation and Restart of a Model Waxy Crude Oil". *Energy & Fuels*, 27:1909–1913.

Macosko, C.W., 1994. *Rheology: Principles, Measurements and Applications*. Wiley-VC.

Pereira, L.G., 2018. *Avaliação experimental do reinício de escoamento de fluidos dependentes do tempo em tubulações*. Dissertation of Master, Federal Technological University of Paraná, Curitiba-PR, Brazil.

Taghipour. A., Lund, B., Sandvold, I., Opedal, N., Carlsen, I., Ytrehus, J. D., Skalle, P., Saasen, A., 2012. "Experimental Study of Rheological Properties of Model Drilling Fluids". *Annual transactions of the Nordic rheology society*, vol. 20.

Tanaka, H., Meunier, J., Bonn, D., 2004. Nonergodic states of charged colloidal suspensions: repulsive and attractive glasses and gels. *Phys. Rev. 49 (031404).*

Tarcha, B.A., Bárbara, B.P., Soares, E.J., Thompson, R.L., 2015. "Critical quantities on the yielding process of waxy crude oils". *Rheol. Acta* 54:479–499.

Venkatesan, R., Nagarajan, N.R., Paso, K., Yi, Y.B., Sastry, A.M., Fogler, H. S., 2005. "The strength of paraffin gels formed under static and flow conditions". *Chem. Eng. Sci*. 60:3587–3598.

Yao, B., Li, C., Yang, F., Zhang, Y., Xiao, Z, Sun, G., 2016. "Structural properties of gelled Changqing waxy crude oil benefitted with nanocomposite pour point depressant". *Fuel* 184:544–55.

7. RESPONSIBILITY NOTICE

The authors are the only responsible for the printed material included in this paper.